Design, Manufacture and Evaluation of Carbon/Epoxy Composite Beams with Embedded SMA Wires for Bending Control

G. Zhou, J. Loughlan and P. Lloyd[+]

Department of Aeronautical and Automotive Engineering, Loughborough University, Loughborough, Leicestershire, LE11 3TU, UK
[+]DSTL, MoD, Farnborough, Hants GU14 0LX, UK

ABSTRACT

Smart adaptive beams with 16-ply quasi-isotropic carbon/epoxy host and 10 nitinol wires prestrained to 5.5% were made in an autoclave with a purpose-made alignment device. The wires were eccentrically embedded in the axial direction. Beams of the same condition were duplicated and beams of different lengths were also made. The bending actuation of these adaptive beams was experimentally evaluated in a cantilever set-up by applying electric current to the nitinol wires. The evaluation showed that the present fabrication process was repeatable and reliable. The induced maximum end deflections of 0.9 mm to 1.8 mm, dependent on beam lengths, seemed to be limited. It was found that this level of the end deflections could be due to limited load transfer from the axial contraction of the wires to bending, which could in turn stem from the small eccentricity.

1 INTRODUCTION

Shape memory alloys (SMAs) such as nitinol have the ability to endure diffusionless solid-state phase transformation and this unique thermomechanical behaviour is characterised by four critical temperatures, thereby being capable of being developed into actuators. SMAs are usually produced in the form of wires and thus are particularly suited for being embedded in the host composite structures, thereby creating adaptive smart structures. Once the embedded prestrained SMA wires are energised through electric heating, their longitudinal contraction is capable of altering a real-time structural shape in a controlled manner, phenomenon called the shape memory effect (SME). One such application area in recent years is to use the SME to control a bending of load-bearing composite structures so as to enhance ultimately their structural performance [1-4]. If the elastic stiffness of the host structures is required to return the deformed structures to their original forms, this phenomenon of the current interest is called the one-way SME, though the two-way SME has also been investigated [5-7].

The bending or shape control usually requires a large energy density with high recovery force along with high deflection. Since the movement of the embedded SMA wires within the host composite is constrained by either uniform bonding along their length or at their ends, the bending of adaptive smart beams can be achieved when the contracting wires are located away from the neutral plane of the beams. Obviously, such bending actuation depends on the level of prestrain, volume fraction and the through-the-thickness location of the wires, and the host flexural rigidity in addition to the level of applied current and ambient temperature. Clearly, these major parameters impose significant conflicting requirements to the multi-cycle actuation performance of the beams. For example, to obtain high energy density, it seems intuitively to be a good idea to embed a large amount of highly prestrained wires in the host beam with a relatively low flexural rigidity which is actuated by a high level of current. However, the high prestraining could lead to rapid ageing of the wires during the multi-cycle actuation [8]. The well-established aeronautical composite host structures must have a flexural rigidity of above certain level, and such flexural rigidity could be favourably transformed to thickness for the greater desired eccentricity. However, the greater flexural rigidity of the host must be overcome to allow bending to be induced and thereby its increase could outweigh the corresponding eccentricity gain. Also a high level of applied current could be desirable for high response rate and constraint-induced overheating is necessary to ensure

the completion of the reverse transformation. Nevertheless, both could certainly result in heat damage in the host resin [8-9]. In addition, embedding too many SMA wires in the host could adversely affect the long-term through-the-thickness mechanical properties of the smart structures [10]. Although the literature abounds with individual endeavours of using SMAs for the shape control of structures [1-4], there is little information on the comprehensive design analysis and guidelines for the performance of the SMA-based adaptive composite structures. In particular, there is little on the study of the load transfer from axial contraction of the wires to bending of the host beams. In the work presented here, various adaptive carbon/epoxy beams containing nitinol wires were designed and manufactured. The bending actuation of these adaptive cantilever beams was examined experimentally with focus on performance characterisation and on actuation repeatability.

2 DESIGN CONSIDERATIONS

The design and manufacture of adaptive beams require the selection of SMA material, prestrain level, volume fraction and through-the-thickness location, host composite material and lay-up, a level of applied current, and beam dimensions for the given performance requirement in terms of bending strain. Then the desired maximum actuation performance of adaptive beams could be obtained through parametric optimisation.

There are three major SMAs such as Cu-Zn-Al, Cu-Ni-Al and binary Ni-Ti (nitinol) used for adaptive structural applications [11-12]. The latter was selected because of its greater recovery capacity, excellent corrosion resistance, stable transformation temperatures with a relatively high electrical resistance and compatibility with a cure temperature of the present host composite. The current nitinol wire has a nickel content of 55.3%. Its transformation temperatures were determined from thermographs generated using a differential scanning calorimetre (DSC) and they are austenitic start temperature A_s of 47^0C, austenitic finish temperature A_f of 55^0C, martensitic start temperature M_s of 21^0C and martensitic finish temperature M_f of 16^0C. A wire diameter of 0.51 mm was selected as the wires of a larger diameter for a constant wire volume fraction had greater recovery force than that of a smaller diameter [13]. It was understood that the greater energy density via the larger diameter wires could be achieved at the expense of slower heating and cooling rates due to their increased mass and thermal capacitance.

Although a 32-ply thick quasi-isotropic carbon/epoxy laminate would provide a more useful flexural rigidity for the host beam as well as a larger eccentricity, its flexural rigidity could be much more difficult to overcome. Thus, a 16-ply carbon/epoxy laminate (T700/LTM45-EL) was used as the host with a stacking sequence of $(+45°/90°/-45°/0°/SMA/0°/-45°/90°/+45°)_S$. The flexural modulus of the intact host laminate beams was measured to be about 47.0 GPa. One through-the-thickness quarter location was selected to provide a large wire eccentricity, although it was very desirable to have the wires embedded as far away from the neutral plane of the beams as possible. Two adjacent plies were oriented to 0° in the longitudinal direction of the beams so that the nitinol wires could partially sink in between them so as to minimise local distortion. Previous experimental investigation for the through-the-thickness mechanical properties of adaptive smart beams confirmed that neither interlaminar shear nor flexural properties suffered substantial degradation [10]. Although the optimum curing temperature of 60°C and a glass-transition temperature of 75°C for the matrix were slightly greater than austenitic start and finish temperatures, nitinol wires were tied up on the wire alignment frame during cure so that potential actuation during composite cure could be minimised and thereby their prestrain would not be affected.

A beam width of 25 mm was selected to allow the maximum number of ten nitinol wires to be embedded side by side with a minimum wire-to-wire spacing of 1.5 mm [10]. As a result, this resulted in the wire volume fraction of about 4.1%. As this level of wire volume fraction is low,

thus slow response rates should be expected. The level of prestrain in the nitinol wires has been measured to be about 5.5% with intention to provide the maximum energy density. This was selected on the basis of a understanding of the fact that if prestrained beyond 6% the wires could risk significant actuation loss via ageing and damage [4,14]. Three different wire lengths were used to examine the effect of response rates associated with the variations of electric resistance, surface area and thermal capacitance.

3 SPECIMEN MANUFACTURE

Each piece of nitinol wires was suspended under a constant load at the side of a 6-m tower before embedment and was trained by cycling it through the transformation temperatures via resistive heating for a total of 25 times [15]. The generation of prestrain was carried out in a similar manner. The wire was suspended again on the tower after training and then was loaded incrementally with dead weights while the corresponding wire elongations were recorded. To end up with the desired plastic prestrain of 5.5%, the wire had to be slightly over-stretched to the strain of about 6% as it contracted slightly when the weights were removed from the wire.

The alignment frame device as shown in Fig. 1 was designed and made to ensure that during composite cure the wires were kept not only longitudinally straight with the desired wire-to-wire spacing but were also at the desired through-the-thickness location. In a few selected beams, K-type thermocouples were also bonded onto the outermost wire with high temperature cement within the host so that the temperature of the embedded wire could directly be measured. Each one was oriented to the direction perpendicular to the nitinol wire at the central section so that its potential separation from the wire was minimised. A total of 16 plies for each adaptive beam were laid up in two separate laminate stacks. The lower stack consisted of 12 plies whereas the upper stack consisted of 4 plies. The entire laminate assembly was cured in an autoclave, following the manufacturers recommended cycle of 60°C at 90 psi for 18 hours.

4 EXPERIMENTAL SET-UP AND PROCEDURE

The nitinol wires in each beam were connected in a series to complete electric circuit via fastening metal ferrules. Each of the adaptive beams was fixed at one end in the cantilever set-up. The deflection of the free end of each beam was measured by a high-precision LVDT with an accuracy of ±0.1 mm. The actual contact location of the bearing ball of LVDT was about 2 mm away from the physical end of each beam. Alternatively, a transverse bending force could also be measured if a load cell was placed in the same position as the LVDT. High-temperature strain gauges (SGs) were bonded on both surfaces of some selected beams. The overall experimental set-up is shown in Fig. 2. In addition to the direct temperature measurement of embedded wire, temperatures of both the beam surface and the protruding part of the nitinol wires of some beams were also measured by thermocouples. To actuate each adaptive beam, electric current of selected level was applied to the nitinol wire via a programmable low-voltage power supply. The duration and the level of current applied to the present adaptive beams were determined through the establishment of a deflection plateau on the deflection-time curves as seen in Fig. 3. The power was disconnected after the estimated deflection plateau was reached. The adaptive beams were either left to cool at room temperature (RT) or placed in a freezer for 2 minutes to ensure a full recovery to M_f of 16°C.

5 RESULTS AND DISCUSSION

Fig. 3 shows a typical end deflection-time curve from a 130-mm long beam (A) with the current of 3.5 amp at 3 volts for the duration of 7 minutes. The initial linear region lasted only up to about 0.35 mm in the first 50 seconds. The rest of the curve exhibits the exponential trend and levelled off

with a plateau which corresponded to the maximum end deflection of 0.89 mm. Although this level of deflection seems small, it could indicate that the bending moment induced by the recovery force was balanced out by the flexural rigidity of the adaptive beam. As the present thick wires were well bonded with the host, the lengthened response time was to some extent expected. When the power was switched off, the nitinol wires cooled exponentially through conduction and convection. The flexural rigidity of the adaptive beam acted as a conventional spring to return the beam to its undeformed position. However, the residual deflection of about 23% maximum end deflection at the end of cooling is visible in Fig. 3, though some tests had much smaller residual deflections (see Fig. 10). This non-zero deflection could be attributed to the following two reasons. One is that the magnitude of residual deflection is close to the sensitivity of the LVDT. The other is that there is difference between M_f of 16°C and ambient (or room) temperature of about 20°C so that the forward transformation was likely to be incomplete. In particular, the actual M_f of the prestrained wires could be less than that with zero prestrain [16]. To verify the latter, a series of tests on the same beam were repeated in an open freezer with ambient temperature of being close to –18°C. Fig. 4 shows comparison of two deflection-time curves, in which the residual deflection of the test with the lower ambient temperature diminished to the only 5% maximum end deflection. This could be attributed to the increased forward transformation during the cooling period. The maximum end deflection somewhat was also reduced by the variation of ambient temperatures. Nevertheless, when both curves were normalised with reference to respective peak deflections, the previous observation is verified in Fig. 5. Indeed, the beam tested in the freezer in Fig. 4 took a little longer time to reach the same deflection in the reverse transformation and a lesser time to cool down. To establish repeatability of the above actuation performance and consistency of the fabrication process, the entire experimentation was repeated with another 130-mm beam (B) fabricated and tested in the same way. In addition, a thermocouple was also embedded in this beam. This second adaptive beam B achieved the maximum end deflection of 0.88 mm at RT with the end deflection-time curves of both beams shown in Fig. 6. Clearly, such repeatable actuation performance from these adaptive beams confirmed that the present fabrication process was very adequate and reliable.

Fig. 7 shows the temperature-time curve of the 130-mm beam B, in which both wire and beam surface temperatures were measured by the embedded and surface-mounted thermocouples, respectively. It can be seen that the wire temperature rose almost linearly to about 195°C in 20 seconds and reached the maximum temperature of about 215°C in 50 seconds. It remained at that level for the rest of the heating period. Clearly, the plateau temperature is nearly four times A_f of 55°C. It implies that much higher temperature and overheating was necessary to complete the reverse transformation for prestrained wires [16] and for larger recovery stress [17-18]. The cooling response was very similar to the heating one, i.e. the wire temperature was back to the initial temperature in a similar time scale. Interestingly, the temperature on the compressive beam surface arose steadily to about 22°C after 50 seconds and reached 40°C only when cooling started. As a nominal distance between the embedded wires and the closer surface was only about 0.25 mm, this seems to indicate that these carbon/epoxy beams were very efficient thermal insulators with the limited ability to dissipate interior heat. If such heating duration was substantial and cyclic, heat damage of epoxy could indeed become an issue. When the above temperature response was plotted against the corresponding deflection as in Fig. 8, it became clear that deflection started only when the stress-free A_f was passed and that major part of deflection took place when the plateau temperature of 25°C was reached.

In the present actuation evaluation of the adaptive beams, the examination of the effectiveness of eccentric axial load-bending transformation is extremely crucial. As the load transfer from contraction of the directly embedded nitinol wires to the host was via interfacial shear, thus the most effective region of the load transfer would be at the free end of the adaptive beams since the

other end was always clamped. And this interfacial shear was likely to decay towards the middle of the beam. Fig. 9 shows strain responses of two back-to-back SGs 26 mm from the clamping end. Interestingly, the strains from both SGs were of compressive nature. The peak values are 230 με from the surface remote to the wires and 455 με from the surface closer to the wires. On the basis of the superposition principle in elementary beam theory, the bending strain at the same location could be only 113 με whereas the compressive axial strain was about 343 με, which was three times greater. This seems to suggest that the compressive axial strain induced by the wire contraction was much greater than the transferred bending strain, and thereby the load transfer was limited.

Beams of two different additional lengths were also tested and their results in Fig. 10 show that both the initial linear regions and the maximum end deflections seemed to be proportional to the length increase of the wires. Although the length increase increases the electric resistance, surface area and thermal capacitance of the wires [19], these effects did not seem to be significant on the response rates of the present adaptive beams.

6 CONCLUSIONS

Adaptive beams with quasi-isotropic carbon/epoxy host and prestrained nitinol wire actuators were made in an autoclave with a purpose-made alignment device. The wires were eccentrically embedded in the axial direction. Beams either of the same condition or with two different lengths were also made. The bending actuation of these adaptive beams was evaluated experimentally in a cantilever set-up by applying electric current to the nitinol wires. Such evaluation showed that the present fabrication process was repeatable and reliable. The induced maximum end deflections of 0.9 mm to 1.8 mm, dependent on beam lengths, seemed to be limited. It was found that this level of the end deflections could be due to limited load transfer from the wire axial contraction to bending. This could in turn stem from the available small eccentricity against the substantial level of the flexural rigidity of the present beams.

Acknowledgement: The authors acknowledge the execution of some tests by Mr A.R. Giles.

REFERENCES

1 Birman, V., Review of mechanics of shape memory alloy structures, *Applied Mechanics Review*, 50 (1997), 629-645.
2 Wei, Z.G., R. Sandstrom and S. Miyazaki, Shape memory materials and hybrid composites for smart system, 33 (1998), 3763-3783.
3 Baz, A., Shape control of composites, in Comprehensive Composite Materials ed. A. Kelly and C. Zweben, Elsevier Science, London, 2000.
4 Chopra, I., Review of state of art of smart structures and integrated systems, *AIAA J.*, 40 (2002), 2145-2187.
5 Hebda, D.A., M.E. Whitlock, J.B. Ditman and S.R. White, Manufacturing of adaptive graphite/epoxy structures with embedded Nitinol wires, *J. of Intelligent Material Systems and Structures*, 6 (1995), 220-228.
6 de Blonk, B.J. and D.C. Lagoudas, Actuation of elastomeric rods with embedded two-way shape memory alloy actuators, *Smart Materials and Structures*, 7 (1998), 771-783.
7 White, S.R. and J.B. Berman, Thermomechanical response of SMA composite beams with embedded nitinol wires in an epoxy matrix, *J. of Intelligent Material Systems and Structures*, 9 (1998), 391-400.
8 Doran, C.J., The effect of prestrain on the actuation performance of embedded shape memory alloy wires, *Proc. of 2nd Euro. Conf. on Smart Structures and Materials*, Glasgow, 1994.
9 Friend, C.M., N.B. Morgan and V.D. Wise, Some durability issues associated with the use of shape-memory alloy 'smart' composites, *Proc. of Mat. Res. Soc. Symp.*, 360 (1995), 513-518.
10 Zhou, G., L.M. Sim, P. Brewster and A.R. Giles, Through-the-thickness mechanical properties of quasi-isotropic carbon/epoxy laminates, *Composites Part A*, in press.
11 Thompson, S.P. and J. Loughlan, Enhancing the post-buckling response of a composite panel structure utilising shape memory alloy actuators–a smart structural concept, *Composite Structures*, 51 (2001), 21-36.
12 Huang, W., On the selection of shape memory alloys for actuators, *Materials and Design*, 23 (2002), 11-19.

13 Epps, J. and R. Chandra, Shape memory alloy actuation for active tuning of composite beams, *Smart Materials and Structures*, 6 (1997), 251-264.
14 Brinson, L.C., M.S. Huang, C. Boller and W. Brand, Analysis of controlled beam deflections using SMA wires, *J. of Intelligent Material Systems and Structures*, 8 (1997), 12-25.
15 Chopra, I., Review of current status of smart structures and integrated systems, *Proc. of SPIE Conf.*, 2717 (1996), 20-62.
16 Stalman, R., Tsoi, K. and Schrooten, J., The transformation behaviour of shape memory wires embedded in a composite matrix, *Proc. of SPIE Conf.*, 4073 (2000), 88-96.
17 Brinson, L.C., A. Bekker and S. Hwang, Temperature induced deformation in shape memory alloys, *Proc. of SPIE Conf.*, 2427 (1995).
18 Elspass, W.J. and J. Kunzmann, Design, manufacturing and verification of laminates with embedded SMA actuators, *Proc. of SPIE Conf.*, 2717 (1996), 320-329.
19 Baz, A., K. Inman and J. McRoy, The dynamic and thermal characteristics of shape memory actuators, *Proc. of SPIE Conf.*, 2190 (1994), 436-453.

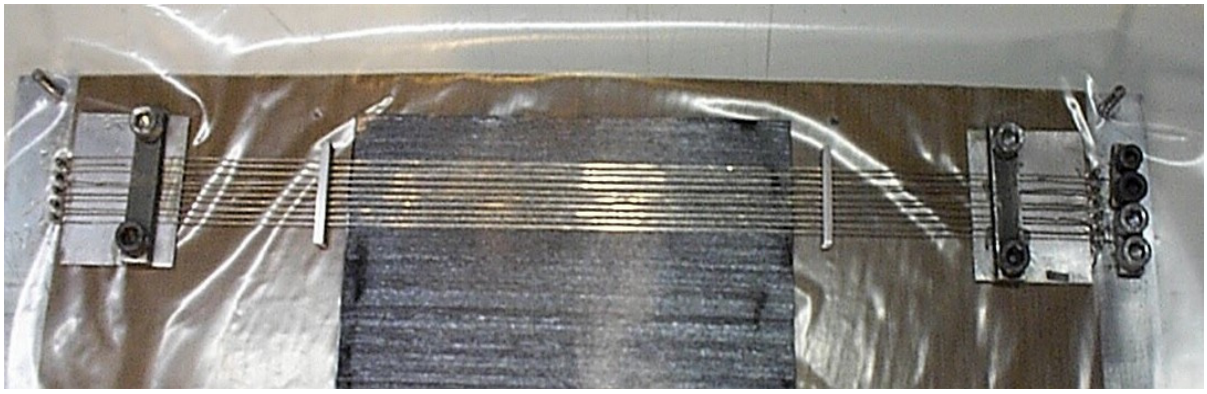

Figure 1 SMA wire alignment device for manufacturing adaptive composite beams

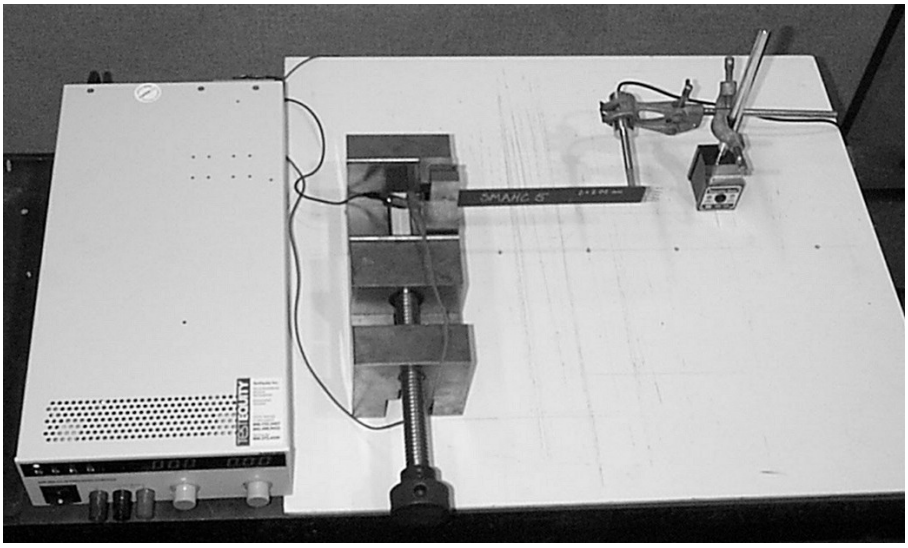

Figure 2 An experimental set-up for actuation of an adaptive beam embedded with nitinol wires

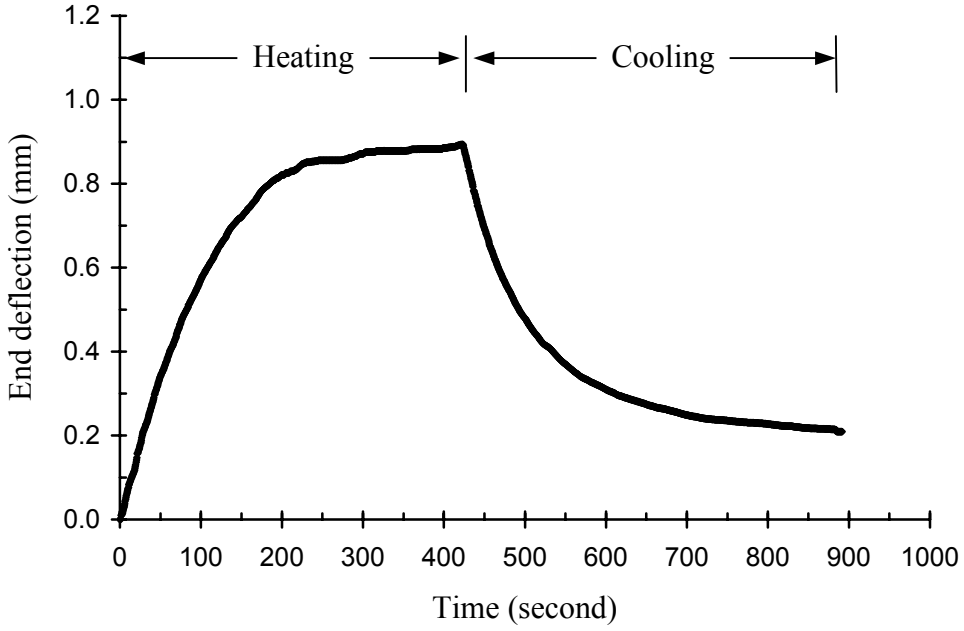

Figure 3 Deflection-time curve from a 130-mm long adaptive beam at RT of 22^0C

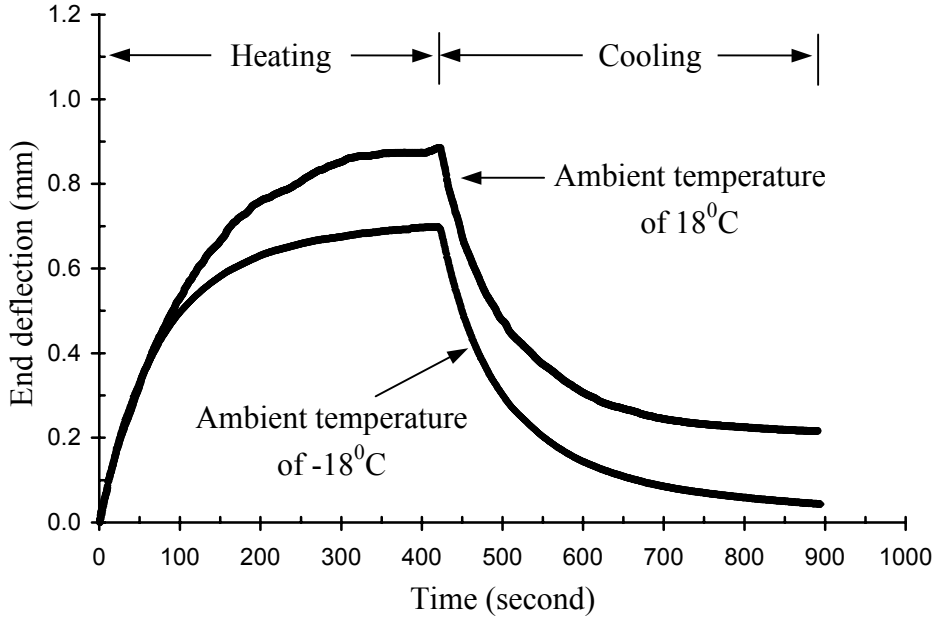

Figure 4 Deflection-time curves from a 130-mm long adaptive beam actuated at two different ambient temperatures

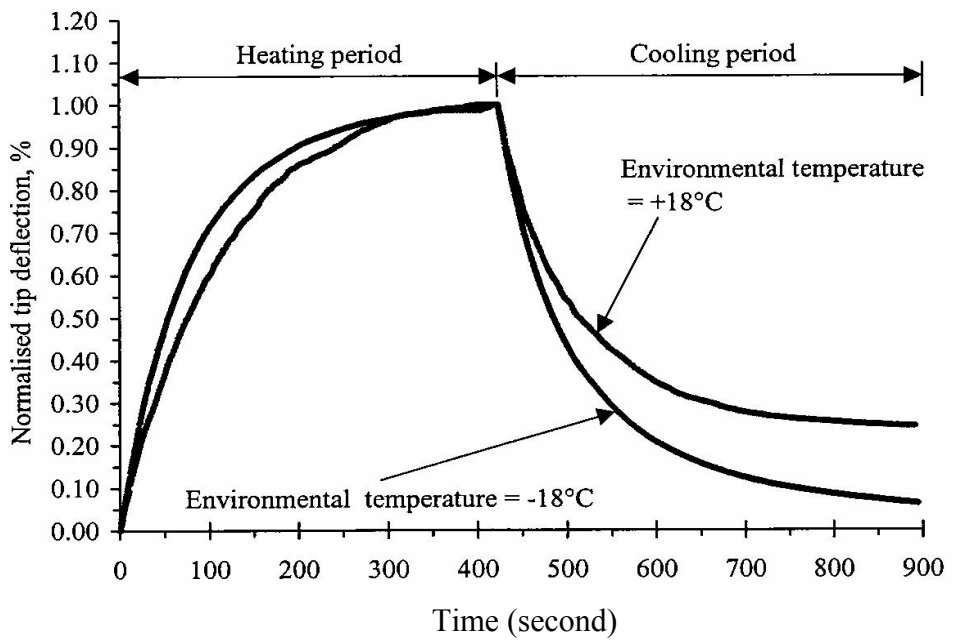

Figure 5 Normalised deflection-time curves from a 130-mm long adaptive beam tested at two different ambient temperatures

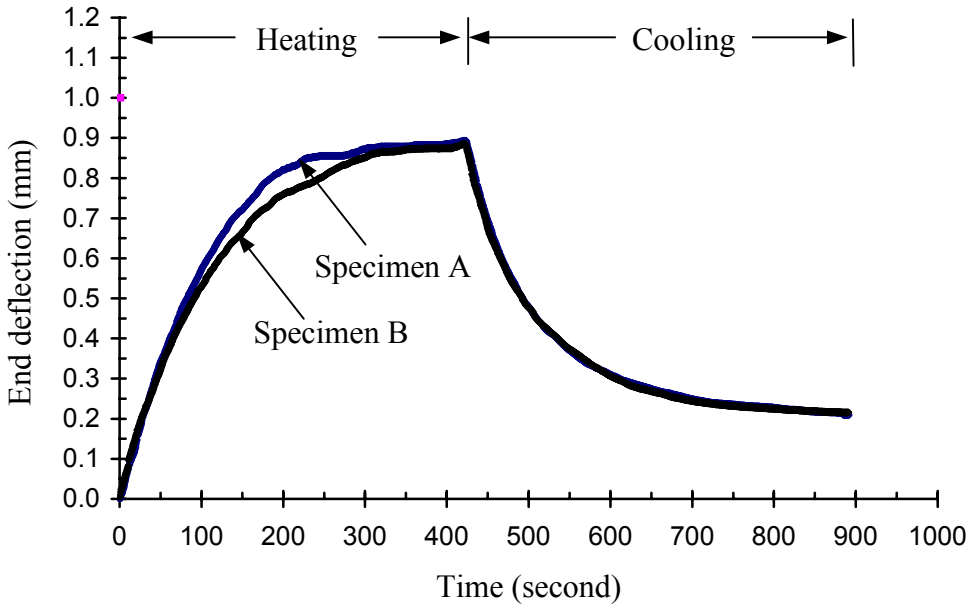

Figure 6 Deflection-time curves from two 130-mm long adaptive beams at room temperature

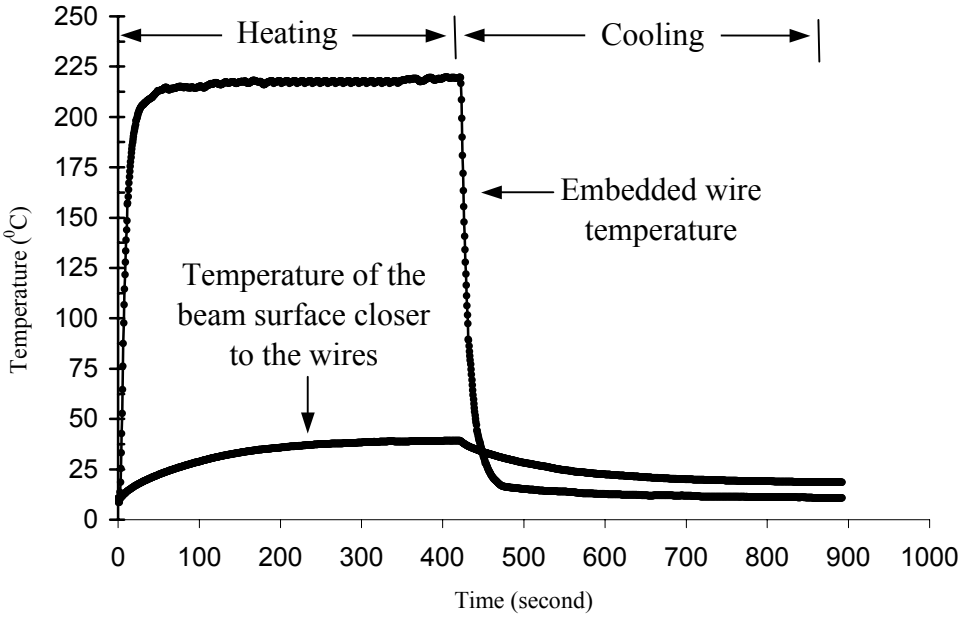

Figure 7 Temperature-time curves from a 130-mm long adaptive beam B at RT

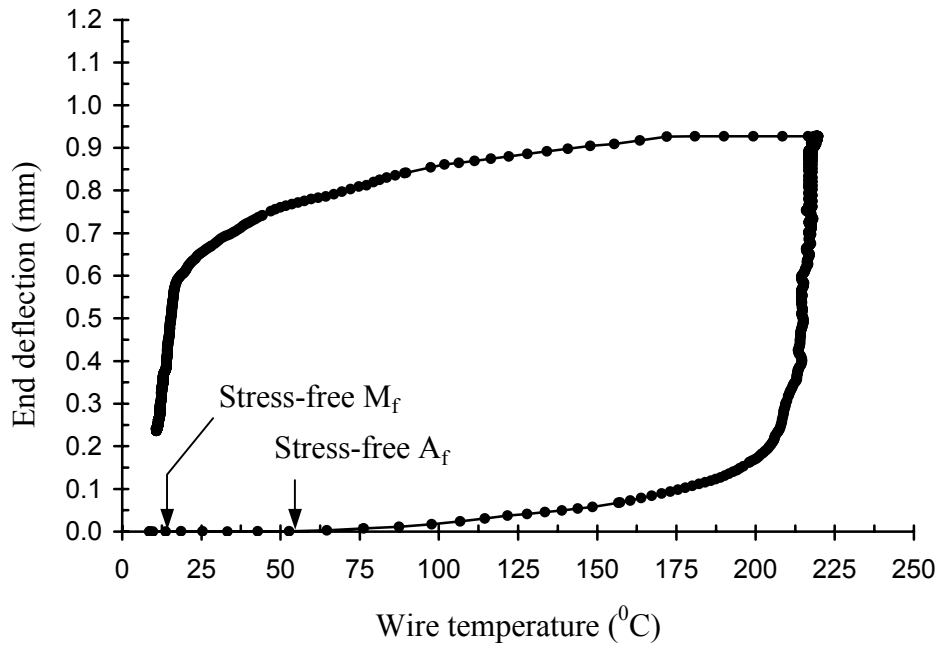

Figure 8 Temperature-time curves from a 130-mm long adaptive beam B at RT

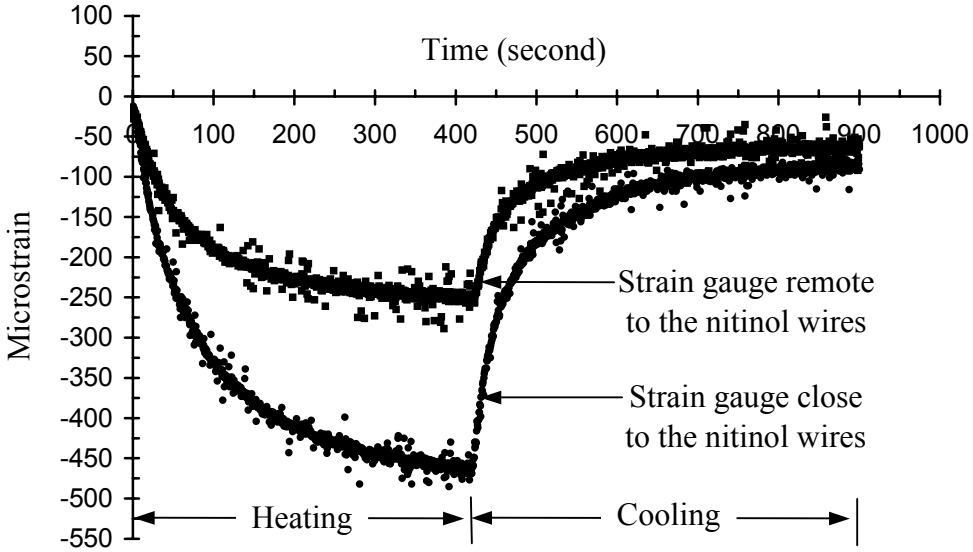

Figure 9 Strain-time curves from a 130-mm long adaptive beam

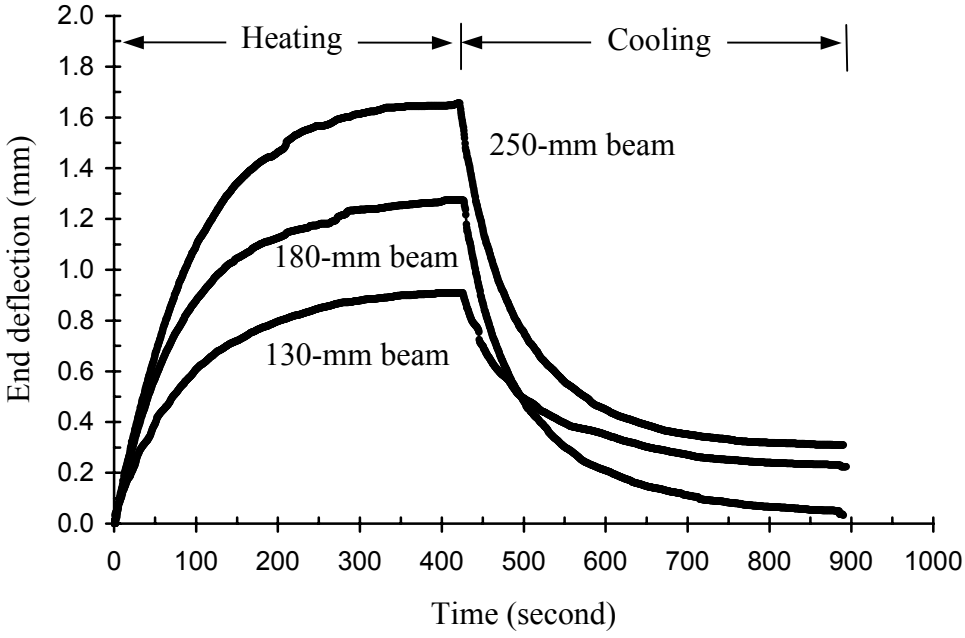

Figure 10 Deflection-time curves from adaptive beams of three different lengths at RT